Early Holocene large-scale meltwater discharge from Greenland documented by foraminifera and sediment parameters

Marit-Solveig Seidenkrantz (1), Hanne Ebbesen (2), Steffen Aagaard-Sørensen (1, 3), Matthias Moros (4), Jeremy M. Lloyd (5), Jesper Olsen (6), Mads Faurschou Knudsen (1), Antoon Kuijpers (2)

1 Centre for Past Climate Studies, Department of Geoscience, Aarhus University, Denmark

2 Geological Survey of Denmark and Greenland (GEUS), Denmark

3 Present address: Department of Geology, Tromsø University, Norway

4 Institute for Baltic Sea Research, Warnemünde, Germany and Uni Bjerknes Centre, Bergen, Norway

5 Department of Geography, University of Durham, UK

6 Centre for Climate, the Environment & Chronology (14CHRONO), Queen's University Belfast, UK

Corresponding author: mss@geo.au.dk / Phone: +45 8942 9454

Abstract

Records of foraminiferal assemblages combined with lithological properties (grain size, magnetic parameters and XRF data) of marine sediment cores from West Greenland coastal waters and the adjacent Labrador Sea document widespread early Holocene meltwater discharge. This discharge is concluded to originate from large-scale melting of the Greenland Ice Sheet (GIS) having started prior to 8,600 cal. yr BP and ended at about 7,700-7,500 cal. yr BP, when the GIS margin had withdrawn from the fjords and become mainly land-based. The benthic foraminiferal record from one of the coastal sites mainly reflects West Greenland Current (WGC) subsurface water properties and to a minor degree surface productivity. The most significant feature in this record is an abrupt shift to a higher-productivity regime around ~7,700 cal. yr BP. We suggest that the cessation of a widespread GIS meltwater discharge at that time favoured an increased influence of (sub)surface water of Atlantic origin and initiation of modern subpolar gyre circulation enabling Labrador Sea deep convection. Further offshore, a record of planktonic foraminiferal assemblages shows an oceanographic change at ca. 9,500 cal. yr BP, while a gradual but marked change in the planktonic foraminiferal assemblage between 8,800-7,000 cal. yr BP may be related to a narrowing of the WGC low-salinity surface water belt. The oceanic regime off West Greenland prior to ~7,800 cal. yr BP was thus characterised by the presence of a permanent and widespread meltwater surface layer, presumably preventing deep convection in this region. Apart from indications of a slight decrease in meltwater discharge by the benthic foraminiferal fauna data, neither of the records shows any clear signal of a regionally important 8.2 ka event.

Keywords: Greenland, early Holocene, meltwater discharge, foraminifera, sediment properties, magnetic susceptibility, 8.2 ka event

1. Introduction

Today we witness how melting of the Greenland Ice Sheet (GIS) has become a very important aspect of understanding the consequences of possible future climatic changes. The rising global average temperature may result in increased ice-sheet melting, a process that can be expected to accelerate in the future (e.g. IPCC 2007). Since 1979, the area of the inland ice influenced by melting has become significantly enlarged (Steffen et al. 2004), and satellite observations inform us that during the last decade, ice discharge from the GIS has led to a substantial increase in the annual ice-sheet mass deficit (Rignot and Kanagaratnam 2006, Nick et al. 2009, Rignot et al. 2011). Studies of ablation rates from ice cores furthermore indicate that GIS ice discharge rates over the last few decades in some areas surpass any rates reconstructed for the last 4,000 years (Mernild et al. 2012). In addition, during the past decades the temperature of the Arctic region has increased twice as much as in the rest of the world (ACIA 2004, AMAP 2009), demonstrating the high sensitivity of the Arctic region to climate change (Overpeck et al. 1997). Thus, the GIS is recognised as an important factor in future climate scenarios, not only because of sea-level rise, but also due to the possible meltwater impact on Atlantic Meridional Overturning Circulation (AMOC), which could eventually lead to marked cooling of the eastern North Atlantic region.

Past climate reconstructions attribute marked regional cooling to the effect of meltwater discharge into the North Atlantic, which may provide a possible analogue for future climate scenarios. For the early Holocene, evidence of such a North Atlantic cooling episode was first discovered in Greenland ice cores (Johnsen et al. 1992, 2001). This ‘8.2 ka cooling event’ has afterwards been recognised at numerous sites in the North Atlantic region (e.g., Klitgaard-Kristensen et al. 1998, Risebrobakken et al. 2003, Rohling and Pälike 2005, Alley and Ágústsdóttir 2005, Came et al.

2007). A generally accepted explanation for the origin of this event is a large-scale freshwater discharge from the Hudson Strait, Canada, where large proglacial lakes drained around 8,200 cal. yr BP, affecting the AMOC (Alley et al. 1997; Barber et al. 1999, Leverington et al. 2002, Hall et al. 2004, Ellison et al. 2006, Came et al. 2007, Kleiven et al. 2008). This also affected global atmospheric conditions, including a lowering of pCO_2 (Wagner et al. 2002). Only limited attention has, however, been given to the possible role of melting of the GIS, which represents the largest ice mass on the Northern Hemisphere since the early Holocene. Here, we study four high-resolution marine sediment records collected in West Greenland waters to test for a possible 8.2 ka event signal in this region and to investigate the potential influence of the GIS on early Holocene meltwater production. Lithology, magnetic susceptibility (MS) and anhysteretic remanent magnetization (ARM) records from three marine sediment cores taken in coastal waters off West Greenland illustrate the sedimentary regime and more specifically indicate the strength of meltwater discharge. For one of these records from Southwest Greenland, we additionally performed a high-resolution benthic foraminiferal study of the subsurface conditions, while the open-ocean conditions are documented by planktonic foraminiferal and stable isotope records from a fourth, deep-water core site in the northeastern Labrador Sea. Our discussions will focus on the early Holocene sections of these records.

2. Modern oceanographic conditions

Today the West Greenland region is mainly influenced by the West Greenland Current (WGC) (Fig. 1). At the surface, the WGC transports cold, low-salinity water masses consisting mainly of glacial meltwater and Polar Water from the East Greenland Current (EGC). At greater water depths (> 150-200 m), the WGC entrains warmer, saline Atlantic water-masses (Irminger Sea Water; ISW)

93 derived from the Irminger Current (IC) (Tang et al. 2004, Cuny et al. 2005). As the WGC flows
94 northward along the West Greenland coast, its polar water component gradually turns westward,
95 allowing the warmer, Atlantic component to rise towards the surface. On the western side of the
96 basin, the Baffin-Labrador Current system transports cold, low-salinity Polar Water south along the
97 Canadian coast.
98
99 **3. Material and Methods**
100
101 Our data derive from four marine sediment cores off West Greenland (Fig. 1; Table 1). Two piston
102 cores, DA00-06P (hereafter DA06P) and DA00-04P (DA04P), were collected during a cruise in
103 2000 with the Danish research vessel *RV Dana* (Kuijpers et al. 2001) from Disko Bugt and
104 Kangersuneq Fjord, respectively (Fig. 1). Piston cores DA04-31P (DA31P) and DA04-41P
105 (DA41P) were obtained in 2004 during another GEUS-organised cruise with *RV Dana* (Dalhoff et
106 al. 2005). DA31P was collected from the adjacent northeastern Labrador Sea, while DA41P is
107 derived from Ameralik Fjord (Lysefjord) in the Godthåbsfjord region (Fig. 1).
108
109 The age control of the sediment cores is based on Accelerator Mass Spectrometry (AMS) ^{14}C
110 measurements carried out on planktonic and benthic foraminifera, mollusc shells and marine plant
111 material at the AMS ^{14}C Laboratory, Aarhus University (Denmark; AAR), the Leibniz-Laboratory
112 for Radiometric Dating and Isotope Research, Kiel (Germany; KIA), Poznan Radiocarbon
113 Laboratory (Poland; Poz) and the Utrecht van der Graaf Laboratorie (the Netherlands; UtC) (Table
114 2). The ^{14}C ages were calibrated using the OxCal v. 4.1 program (Ramsey, 2008) and the marine
115 calibration curve Marine09 (Reimer et al. 2009). Local reservoir ages, ΔR, have been used for sites
116 where ΔR information was available (Reimer and Reimer 2001, Table 2). To our knowledge,

information on local reservoir age variability for the Labrador Sea (DA04-31P) is non-existing and a local reservoir age of $\Delta R = 0 \pm 100$ has therefore been used for the Holocene and $\Delta R = 0 \pm 150$ for the pre-Holocene, i.e. a standard 400-year reservoir age with an uncertainty of the reservoir age of 100 years thus taking the general uncertainty of the reservoir age in the region into account (Fig. 2, Table 2). Age models were constructed using depositional models in OxCal with k values between 50 and 100, yielding A_{model}>95% for all sites. Where changes in sedimentation rate in the cores occur, these have been placed at sedimentological and/or faunal boundaries when consistent with the age model. For DA06P, an outlier model was further applied. In core 31P, the onset of the Holocene at 55 cm (11,703 ±50 b2k), the Younger Dryas (12,896 ±69 b2k) and the Bølling (14,692 ±93 b2k) were also used (Knutz et al. 2011). The above approach has resulted in a slight change in age model compared to those previously published by Lloyd et al. (2005; DA00-06P), Knutz et al. (2011; DA31P) and Ren et al. (2009; DA41P), which all used different approaches based on linear interpolation between dating points. Cores DA06P, DA04P, and DA31P encompass the entire Holocene, whereas a hiatus, or markedly reduced sedimentation rates, is found in core DA41P (ca. 7,400-4,400 cal. yr BP) (Ren et al. 2009; Fig. 2). For lists of ^{14}C-dates and details on age models see Table 2 and Lloyd et al. (2005; DA00-06P), Knutz et al. (2011; DA31P), Ren et al. (2009; DA41P). All ages referred to below are given as calibrated years before present (cal. yr BP), where BP equals 1950 AD. The age models are shown for the entire cores but the proxy data relevant to this study will here be limited to the early Holocene sections.

Magnetic susceptibility (MS) measurements were carried out on three cores (Figs. 3, 4). The measurements were performed on split halves of the cores using continuous 2x2x2 cm plastic boxes at c. 2.25 cm intervals. The initial magnetic susceptibility (measured as mass specific magnetic susceptibility (χ) in 10^{-6} m^3kg^{-1}) of the subsamples was measured at Lund University using a

Geofyzica Brno KLY-2 Kappabridge. Anhysteretic remanent magnetization (ARM) was measured with a Molspin Minispin magnetometer and divided by the DC bias field to provide the mass specific susceptibility of ARM (χ_{ARM}) (in 10^{-6} m^3 kg^{-1}). The χ_{ARM} / χ ratios generally reflect the grain size of the magnetic mineral fraction; the use of magnetic parameters in palaeoceanographic studies has been widely discussed in the literature (e.g., Verosub and Roberts 1995, Stoner and Andrews 1999, Snowball and Moros 2003).

XRF core scan data from core 41P are described by Ren et al. (2009). The bulk geochemical composition was determined at the Royal Netherlands Institute for Sea Research, Texel, using an X-ray fluorescence (XRF) core scanner (Jansen et al. 1998) in 1-cm steps and reported as counts per second (cps). The intensity of the elements Fe, Ti, K, Ca and Br are included here (see also Ren et al. 2009). Grain sizes were obtained by use of wet sieving through mesh sizes of 0.063 and 0.100 or 0.150 mm.

Detailed benthic foraminiferal analyses were carried out on core DA41P (no or few planktonic foraminifera were present in the samples) at high resolution (Fig. 5). Except for the bottom part of the core containing low foraminiferal abundances, sub-samples for foraminiferal analyses were studied at 1-10 cm intervals with the main part of the relevant section studied at 1-5 cm resolution providing an average time resolution of 6.4 years for the section presented here; each cm of sediment comprises between 0.17 and 2.2 years. Planktonic foraminifera were analysed in DA04-31P (Fig. 6) at 0.5-10 cm intervals, generally giving a time resolution of 100-300 years. Each sample represents a 1cm slice of a core section. After weighing, the dried samples were immersed in a 5% solution of H_2O_2 for approximately 20 minutes. Subsequently, the samples were wet-sieved using mesh sizes of 1.0, 0.1 and 0.063 mm and they were further disintegrated using a peptizising agent ($Na_4P_2O_7$, $10H_20$). For a few samples only, it was necessary to concentrate the foraminifera

through heavy liquid CCl_4 (density 1.66g/cm^3). Only foraminifera in the 0.1-1.0 mm fraction were analysed. The 0.063-0.1 mm fraction yielded no species that were not also present in the 0.1-1.0 mm fraction and the >1.0 mm fraction was barren for foraminifera. The foraminifera were relatively well-preserved, and the occurrences of abrupt, significant changes in the faunas indicate that reworking and bioturbation were negligible. To obtain a statistically qualified dataset, we aimed at analyzing at least 300 benthic foraminifera in each sample, but a minimum of 60 specimens for one sample was accepted. Due to the loss of some counts after percentage calculation, the frequency of *Cassidulina neoteretis* cannot be shown for all samples. The flux of foraminifera was calculated assuming a mean sediment density of 1.89 g/cm^3.

Oxygen and carbon isotope measurements of the planktonic species *Neogloboquadrina pachyderma* (sinistral) (core DA04-31P; Fig. 6) were performed on a Finnigan MAT252 mass spectrometer at Woods Hole Oceanographic Institution (WHOI) following the procedure described by Ostermann and Curry (2000). All values are calibrated to the PDB scale.

4. Results and palaeoenvironment

4.1. Greenland glacier retreat and meltwater production

The bedrock and thus the main provenance of the sediments at all three coastal sites (DA06P, DA04P, DA41P) consists of gneiss, while Cretaceous and Paleogene sedimentary strata and basalts are found on Disko Island and in parts of Disko Bugt (McGregor 1993; Henriksen et al. 2009). Except for the χ_{ARM}/χ ratio from DA41P, the MS records from these three coastal sites show a general decrease from high values in the earliest part of the study period to considerably lower

values later, i.e. at around 7,700-7,500 cal. yr BP (Figs. 3, 4). For DA04P and DA06P the same is true for the χ_{ARM}/χ-ratio (Fig. 3), whereas the χ_{ARM}/χ-ratio in DA41P differs (Fig. 4). MS values depend on the content of magnetic grains but also on the grain size and mineralogy of the sediment (e.g. magnetite has a stronger signal than hematite). Generally, the MS signal is high in "glacier milk" (meltwater plume) deposits due to its high contents of hematite and it seems to be strongly linked to Fe in core DA41P. In contrast, χ_{ARM}/χ ratios reflect more specifically the grain size of the magnetic mineral fraction (Moros et al. 2006) and are not simply linked to Fe. The XRF data from core DA41P show higher values of Iron (Fe), Potassium (K) and Titanium (Ti) (Fig. 4) prior to ca. 7,750 cal. yr BP. Fe, K and Ti are common elements in the bedrock surrounding the site (Steenfelt 1990), and may thus be used as indicators of terrestrial influence (Møller et al. 2006). Concurrently, fine-grained sediments (<0.063 mm sediment grain size) are found prior to ~7,700 BP in cores DA04P and DA41P (Figs. 3, 4), again dropping to lower values after ~7,550 BP in DA41P. A shift in magnetic grain size (χ_{ARM}/χ) in core DA06P at ca. 7,500 BP (Fig. 3) is coeval with the shifts in sediment seen in DA04P and DA41P within 2σ errors, but the slightly later change may also be due to its closer proximity to the glacier. In general, the grain-size signal is less clear in core DA06P (Fig. 3). This may in fact be linked to its close proximity to the Jacobshavn Isbrae, which even today continues to exert strong influence on sediment deposition at this site, most notably with fine-grained sediments derived from meltwater plumes and coarser grains transported by icebergs.

All of these data indicate significant meltwater release from Greenland from at least as early as 8,600 cal. yr BP (core DA06P) until ca. 7,700±50 cal. yr BP (cores DA04P and DA 41P; 7,500 cal. yr BP in core DA06P) with a fine-grained unit marking deposition from large meltwater plumes. At relatively glacier-distal sites, meltwater plume deposits are typically characterized by structureless, homogeneous clays and silts (Dowdeswell and Cromack 1991), rich in hematite and goethite as

indicated by mineral magnetic parameters (I. Snowball, pers. comm. 2011), having accumulated at high sedimentation rates. As the ice retreated further towards land, the sediment grain size increased, suggesting a reduction of the meltwater plume possibly combined with a thinner surface meltwater layer and stronger bottom current activity, as also indicated by the increased frequencies of the benthic foraminifera *A. gallowayi* and *C. lobatulus* in core DA41P (Fig. 5). In the uppermost part of core DA41P, the coarser grained sediments again disappeared (Fig. 4), indicating a mainly land-based GIS margin and overall reduction in iceberg calving. A detailed analysis of core DA41P with the highest sedimentation rates documents that the decrease in meltwater discharge extended over a period of about 60 years from c. 7,760-7,700 cal. yr BP (Fig. 4). The complete transition to mainly land-based ice took, however, more time and continued until ca. 7,560 cal. yr BP.

The pattern arising from our core data thus indicates an initially fast ice retreat from the shelf to the coastal region and later further inland within a period of few hundred years. This episode represents the final stage of the deglaciation of the South and West Greenland shelf after the glacial period. Previous studies have dated a deglaciation of the West Greenland shelf at ~9-11,000 cal. yr BP (Knutz et al. 2011), with the ice reaching land about 10-11,000 cal. yr BP (Bennike and Björck 2002; Funder et al. 2004; Roberts et al. 2009; Long et al. 2011). Our data provide a more precise dating of the time (7,700-7,500 cal. yr BP), when the glaciers presumably no longer reached the fjords. However, as indicated by the studies referred to above, much of the surrounding land may have been deglaciated already prior to this time.

4.1.West Greenland Current palaeoceanography

The change in sediment composition in core DA41P was both preceded and accompanied by major changes in the benthic foraminiferal fauna. It is here noteworthy that the sill depth of about ~120 m of the Ameralik Fjord (Fig. 1) implies that the benthic foraminifera at this site reflect WGC subsurface conditions. The water depth at the sill notably represents the depth stratum of the upper boundary of the WGC Atlantic-derived (ISW) water masses. The lowermost part of the record contains only scant benthic foraminifera, which may be linked to a high meltwater supply from land (see above). After ca. 8,250 cal. yr BP the fauna was dominated by *Cassidulina reniforme, Cibicides lobatulus, Elphidium excavatum* f. *clavata* and *Astrononion gallowayi*, but with a characteristic component of *Melonis barleeanus* and *Stainforthia loeblichi* (Fig. 5). Dominance of the benthic foraminiferal species *E. excavatum* and *C. reniforme* indicates a glaciomarine, cold and unstable environment at the seafloor (Steinsund et al. 1994, Korsun and Hald 2000), and the presence of *S. loeblichi* supports the presence of sea ice (Steinsund et al., 1994) as was also suggested by the diatom assemblage (Ren et al. 2009). However, the presence of *M. barleeanus* as well as the common occurrence of high-energy species *C. lobatulus* and *A. gallowayi* (Rytter et al. 2002) indicate that a relatively strong influence of the WGC, entraining a significant ISW component, compensated the outflowing meltwater. *C. neoteretis,* which, despite its low numbers, may be considered a certain indicator of chilled Atlantic water (Seidenkrantz, 1995), indicates a further increase in influx of WGC/ISW water to this site after ca. 7,950 cal. yr BP.

Concurrently with the major changes in MS and grain size values (~7,750 cal. yr BP), *C. reniforme*, and *E. excavatum*, f. *clavata* became less abundant. In contrast, concentrations of *A. gallowayi*, *N. labradorica* and *G. auriculata arctica* increased together with a general rise in benthic foraminiferal flux (Fig. 5). Furthermore, the amount of Calcium (Ca) and Bromium (Br) increased (Fig. 4). With gneiss making out most of the bedrock in the area, no widespread Calcium-bearing rocks are found

261 in the proximity of the cores (McGregor 1993; Henriksen et al. 2009), and both Ca and Br may
262 therefore here be considered indicators of marine biological productivity (Ren et al. 2009). The high
263 frequencies of *Nonionellina labradorica* indicate that this high-productivity period was, amongst
264 others, linked to a nearby location of an oceanic polar front (Hald and Steinsund, 1992; Rytter et al.,
265 2002) as the lower meltwater release from GIS would have allowed further penetration of WGC
266 water into the coastal regions and fjords of West Greenland. After ca. 7,550 cal. yr BP, bottom
267 currents weakened and high frequencies of *Brizalina pseudopunctata* and *Pullenia osloensis* (Fig.
268 5) indicate reduced bottom-water oxygenation.
269
270 Surface-water conditions in core DA41P were studied by Ren et al. (2009), who identified a
271 corresponding major shift in diatom composition with an increase in the warm Atlantic-water
272 indicator *Thalassionema nitzschioides* and a decline of the sea-ice species *Fragilariopsis cylindrus*
273 in the period 7,800-7,600 cal. yr BP; this shift can now be more precisely dated to 7,720 cal. yr BP
274 using our new age model.
275
276 The planktonic foraminifera from the adjacent, open northeastern Labrador Sea (deep-water core
277 DA31P) were generally dominated by the polar species *Neogloboquadrina pachyderma* (sinistral)
278 during the entire study period (Fig. 6). However, relatively high frequencies of *Turborotalita*
279 *quinqueloba* are found prior to ~8,800 cal. yr BP. This is a species known to bloom in areas close to
280 oceanic fronts (Johannesen et al. 1994). This indicates that the oceanic front between WGC water
281 and the polar waters of the central Labrador Sea, which today is found east of the DA31P site, may
282 at that time have been located closer to core DA31P, i.e west of its present location and further from
283 the Greenland coast. Percentages of the warmer-water species *Neogloboquadrina incompta (=N.*
284 *pachyderma* dextral, Darling et al. 2006, Be´ and Tolderlund 1971) were lower around 8,000 cal. yr

285 BP, while *N. pachyderma* (sinistral) increased (Fig. 6). At the same time fluxes of planktonic
286 foraminifera were reduced. Stable oxygen isotope values remained relatively unchanged after ca.
287 9,500 cal. yr BP. In contrast, carbon isotopes show a clearer overall shift to heavier values at about
288 8,800 cal. yr BP, concurrent with the first decrease in *T. quinqueloba* and increase in *N.*
289 *pachyderma* (sin). This suggests more stable stratification and surface water cooling presumably
290 related to enhanced meltwater influx.
291
292 **5. Discussion**
293
294 The magnetic records from the studied coastal sediment cores (Figs. 3, 4) reflect lithological
295 variations, with high values of MS and/or χ_{ARM}/χ here being indicative of terrestrially-derived
296 minerals as also supported by grain sizes and XRF data (Møller et al. 2006, Moros et al. 2006,
297 Seidenkrantz et al. 2007, Ren et al. 2009). Meltwater plumes represent the main source for
298 terrestrially-derived sediments in this region, and the MS records may thus in our study area be
299 used as an indicator of Greenland Ice Sheet (GIS) meltwater discharge in the sense that high MS
300 values in relation to massive silty clay and silt units reflect deposition of suspended matter
301 associated with extensive meltwater plumes from the GIS. In fact, on visual inspection all three
302 cores show massive silt deposition especially associated with the maximum MS values in the early
303 Holocene (Figs. 3, 4) from before 8,600 cal. yr BP onwards (core DA06P; Fig. 3). This points to
304 strong and widespread meltwater discharge at that time. The excessive meltwater production in the
305 early Holocene corresponds to findings by Rinterknecht et al. (2009), who reported a general and
306 fast thinning of the western margin of the GIS in the order of 240 m having occurred between about
307 12,300 cal. yr BP and 8,300 cal. yr BP. A significant GIS retreat during this period is also indicated
308 for the Nares Strait region (England 1999, England et al. 2006), while Fagel et al. (1997) observed a

minimum in smectite suggesting a shorter-term intensified supply of meltwater from the South Greenland margin. The maximum meltwater discharge appears to have decreased near synchronously when comparing the sites from Disko Bugt (DA06P and DA04P) with that from Ameralik Fjord near Nuuk (DA41P). By ca. 7,700-7,500 cal. yr BP, meltwater production had drastically decreased, presumably related to an onshore retreat of the GIS to the coastal margins. Decreased GIS melting and thinning of the surface meltwater layer allowed increased deposition of coarser-grained sediments and stronger bottom current activity (Fig. 5). The marked synchronicity of this decrease in meltwater output may not only characterise the early Holocene retreat and GIS melting history of the West Greenland coastal area, but may be characteristic for the entire sector of Greenland coastal waters affected by warm, saline (subsurface) waters derived from the Irminger Current (IC). A marked intensification of this current system has been reported from Icelandic waters to have occurred at ca. 7,800 cal. yr BP (Castañeda et al. 2004; Olafsdottir et al. 2010), and an associated increase in coarser IRD deposition is documented in sediment records from the Southeast Greenland shelf (Kuijpers et al. 2003). By 6,800 cal. yr BP, the IC had penetrated far north into ocean waters north of Iceland (Jennings et al. 2011).

Benthic foraminiferal faunas from core DA41P from Ameralik show that the West Greenland Current (WGC) was already active at 8,400 cal. yr BP, but with Atlantic-derived waters having less influence prior to 8200 cal. yr BP at the DA41P coring site. The marked decrease in meltwater runoff shown in the MS and XRF records at ca. 7,700 cal. yr BP (Fig. 4), was accompanied by a further strengthening of the inflow of WGC water of Atlantic (ISW) origin into the fjord as shown by the drop in *E. excavatum* and *C. reniforme* and increased abundance of *C. lobatulus* and *A. gallowayi*, indicating higher bottom current activity. This is supported by virtue of the Atlantic-water indicator *C. neoteretis*, which was still present. This increased inflow of WGC water may

thus, amongst others, be linked to a retreat of originally marine-based glaciers causing a reduction in meltwater discharge. The accompanying increase in *G. auriculata, N. labradorica* and benthic foraminiferal flux as well as the higher intensities of Br and Ca after 7,750 cal. yr BP, suggest higher food availability, probably through increased primary production linked to this increased inflow of Atlantic-source water from the WGC. An increased inflow of WGC water is also supported by the diatom assemblage (Ren et al. 2009). Following the end of the high-productivity event at ca. 7,550 cal. yr BP, the benthic foraminifera indicate a reduction of bottom-water oxygenation and reduced bottom current speeds. This implies a shift to more locally influenced conditions and a somewhat reduced inflow of WGC water into the fjord, presumably associated with a continued weakening of the out-flowing meltwater along the surface. This may be linked to a weaker Greenland High and a weaker Subpolar Gyre as suggested by IC changes recorded east of Greenland (Jennings et al 2011).

The planktonic foraminiferal record from the northeastern Labrador Sea (core DA31P; Fig. 6) supports the scenario of a large-scale meltwater episode affecting waters around Greenland in the early Holocene. The drop in planktonic $\delta^{18}O$ concurrent with the peak occurrence of *T. quinqueloba* between ca. 9,500 and 8,800 cal. yr BP may be due to slightly reduced surface water salinity. Relatively high frequencies of *T. quinqueloba,* known to bloom in areas close to oceanic fronts (Johannesen et al. 1994), suggests that the oceanic front between WGC water and the polar waters of the central Labrador Sea was close to this site, i.e. much further west than its present location. This may be attributed to increased GIS meltwater release leading to expansion of the entrained WGC low-salinity surface layer. The following increase in *N. pachyderma* (sin) and decrease in *T. quinqueloba* and *Globigerina bulloides* at ~8,800 cal. yr BP may be caused by a decrease in sea-surface temperature in the northeastern Labrador Sea (Fig. 6) and more stable stratification. A more

357 stable stratification around 8,000 cal. yr BP leading to decreased productivity is also suggested by
358 lowered planktonic foraminiferal fluxes. In addition, this episode also yields some evidence of a
359 short-term intensified cooling suggested by a minimum percentage of *N. incompta*. Whether these
360 relatively short-term changes may be related to the '8.2 ka cooling event' would need further study.
361 The more stable conditions after ~7,000 BP are in agreement with a Labrador Sea oceanographic
362 regime marked by deep convection (see Hillaire-Marcel et al. 2001).
363
364 Evidence for a marked glacier retreat and an associated enhanced meltwater production prior to
365 8,400 cal. yr BP has also been identified in adjacent regions in the Arctic, in particular from the
366 Nares Strait region (Mudie et al. 2004/2006; England et al. 2006). Such a high GIS meltwater
367 output, possibly causing a widespread thick and cold, low-salinity meltwater surface layer offshore
368 South and West Greenland and northeastern Canada from well before 8,200 cal. yr BP to shortly
369 after that time, may also explain the significantly delayed start of the Holocene Thermal Optimum
370 around Hudson Bay (until ca. 7,000 cal. yr BP) when compared with Alaska and northwest Canada
371 (Kaufmann et al. 2004, Keigwin et al. 2005). This scenario is supported by studies concerning
372 Labrador Sea Water formation (Hillaire-Marcel et al. 2001) showing that Labrador Sea deep
373 convection did not take place before ca. 7,500 cal. yr BP, when also the western branch of the North
374 Atlantic Drift may have become strengthened (Andersen et al. 2004). North of Iceland a similar
375 strengthening of the northern branch of the IC was initiated at ~7,800 cal. yr BP (Castañeda et al.,
376 2004; Olafsdottir et al. 2010).
377
378 Despite the high GIS meltwater release indicated by our data, the relatively warmer and saline ISW
379 entrained at subsurface depths by the WGC thus influenced the Greenland coast already prior to
380 8,300 cal. yr BP (Lloyd et al. 2005), with the ISW component proportionally increasing after ca.

7,700 cal. yr BP. This also confirms the conclusions by Knudsen et al. (2008) who found that significant Atlantic Water influence occurred in the Nares Strait well before 8,200 cal. yr BP. In fact, 'warm' ISW entrained by the WGC may have played an important role in its contribution to subglacial melting of the floating glaciers and deglaciation of the West Greenland fjords and coastal waters. A combination of an active WGC and high GIS meltwater discharge may reflect the state of an intensified subpolar gyre circulation as suggested for the 8.2 ka event (Born and Levermann 2010). Based on model simulations, these authors suggest that the freshwater release stabilised the gyre through internal feedbacks causing an intensification of deep-water formation in its centre.

The 8.2 ka event is clearly identified in central GIS ice cores (e.g., Alley et al. 1997; Kobashi et al. 2007). However, apart from a possible slight increase in the >150 µm grain size fraction in core DA06P (8,400-8,100 BP; Fig. 3), possibly due to increased ice-rafting, neither of our records show an actual cooling episode around the well-known 8.2 ka event, even though several of the cores yield a sufficiently high resolution for potential detection of this event. Our data thus imply that the GIS was subject to strong melting already prior to the 8.2 ka event and that this meltwater discharge into Greenland coastal waters continued until about 7,700±50 cal. yr BP. Exposure dating may, however, indicate a stagnating ice front at ~8.3 ka near Kangerlussuaq (Rinterknecht et al. 2009). Although a marked change in GIS melting around 8,200 cal. yr BP affecting West Greenland coastal hydrographic conditions could not be found, we do observe some support for the findings by Rinterknecht et al. (2009) as the increase in benthic foraminifera in DA41P just prior to 8,200 cal. yr BP suggests a slight decrease in meltwater release. This meltwater reduction may have facilitated an increased influx of more saline WGC water into the fjord. The XRF and MS data from this core do, however, not indicate a more substantial change in meltwater discharge.The slight increase of the >150 µm (IRD) sediment fraction in DA06P may be due to a thinning of the surficial meltwater

405 layer favouring iceberg bottom melting, but may also be related to the reduction in meltwater
406 discharge causing a lower sedimentation rate as suggested by the age model (Fig. 2). Furthermore,
407 our data do not completely rule out the possibility that the 8.2 ka event caused a change in ocean
408 conditions further offshore West Greenland. Thus, as also previously concluded for the Disko Bugt
409 area by Long et al. (2006), the 8.2 ka event made only a minor imprint on the GIS melting pattern
410 in the region, if any.
411
412 A similar conclusion was drawn based on sediment cores from along the eastern margin of North
413 America, including the Hudson Strait. These cores did not show any evidence for a change in the
414 surface and deep ocean environment around the 8.2 ka cold event (Keigwin et al., 2005). These
415 sites can be expected to have been directly affected by a freshwater discharge from the glacial lakes
416 in North America. In the Spitsbergen region, sea-surface temperatures (Sarnthein et al. 2003;
417 Ebbesen et al. 2007) show a significantly earlier cooling, presumably related to a southward
418 expansion of Arctic Water masses already at 8,800 cal. yr BP (Ebbesen et al. 2007). This cooling
419 thus spans a much longer period than the relatively short 8.2 ka event. North of Iceland, the cooling
420 event was recorded as an episode of minor amplitude (Castañeda et al. 2004; Jennings et al. 2011),
421 whereas off East Greenland it is only observed as a very minor excursion in carbonate flux
422 (Jennings et al. 2002). In fact, the 8.2 ka cooling event has only been found as a clear spike in
423 certain areas of the North Atlantic that are directly influenced by the North Atlantic Current (e.g.,
424 Came et al. 2007, Sachs 2007, Kleiven et al. 2008), but its signal is virtually absent in those areas
425 mainly influenced by the EGC, WGC, or Baffin-Labrador Current systems (Keigwin et al. 2005,
426 Sachs 2007), or in the high-Arctic Spitsbergen region (Ebbesen et al. 2007). These latter areas are
427 all characterised by the permanent presence of a low-salinity, cold, often ice-loaded, surface water

layer, which may prevent recording of a cooling event that is observed elsewhere in the North Atlantic.

Thus, our results indicate that meltwater and low-salinity water masses expanded in both the Greenland and Spitsbergen regions prior to 8,200 cal. yr BP. This may be related to the early Holocene warming of the circum-Arctic region, including Greenland (Kaufmann et al. 2004), which led to enhanced GIS and glacier melting around the Arctic. Subsequent marked freshening of the EGC and WGC systems as well as the B-LC region led to slowdown of high-latitude deep convection and thus contributed to North Atlantic cooling. In turn, major freshwater release peaking at about 8,200 cal. yr BP may subsequently have triggered internal ocean feedback processes leading to enhanced subpolar gyre convection (*cf.* Born and Levermann 2010). A stronger WGC with a proportionally increased ISW component eventually, i.e. after 7,700 cal. yr BP, led to a Labrador Sea subpolar gyre regime favouring deep convection. In summary, we propose that large-scale melting of the GIS may have significantly contributed to a lowering of North Atlantic surface salinity prior to 8,200 cal. yr BP. The fact that the West Greenland melting pattern seems virtually unaffected by the 8.2 ka event indicates, however, that the GIS was probably not a main driver for this event.

6. Conclusions

We have analyzed early Holocene sedimentary records from West Greenland coastal waters in order to test the possible role of the Greenland Ice Sheet (GIS) for meltwater production during this period. Special attention has been paid to the time around the well-known North Atlantic 8.2 ka cooling event (e.g., Klitgaard-Kristensen et al. 1998, Risebrobakken et al. 2003, Rohling and Pälike

2005). This event has been attributed to effects of a massive freshwater discharge from the Hudson Strait (Barber et al. 1999, Leverington et al. 2002).

Our data from three sedimentary records collected from the Greenland shelf region document high MS and in parts elevated χ_{ARM}/χ values related to massive silt deposition. This is ascribed to deposition associated with large-scale meltwater plumes from the GIS over a longer period spanning the centuries before 8,200 cal. yr BP (earliest indications occurring approximately 8,600 cal. yr BP), and ending after ca. 7,700 cal. yr BP. XRF trace-element composition and foraminiferal faunas from one of the cores provide additional evidence for excessive meltwater production, which can be related to early Holocene warming of the circum-Arctic region including Greenland. Planktonic foraminiferal fauna data from a deep-water site further offshore in the northeastern Labrador Sea indicate widespread presence of negative salinity anomalies reaching far offshore Greenland. Significant freshening of surface waters around Greenland already prior to 8,200 cal. yr BP can be expected to have led to a slowdown of deep-water formation and, in turn, a relatively weak Meridional Overturning Circulation during the early Holocene.

Our data indicate initiation of a modern Labrador Sea subpolar gyre system and West Greenland Current (WGC) configuration at about 7,700 cal. yr BP, leading to regional deep convection shortly after that time as previously reported by other authors (e.g., Hillaire-Marcel et al. 2001). This notably does not exclude the existence of a WGC prior to that time, and our data indeed indicate the presence of an early, strong WGC. This current probably played a major role in the deglaciation of the West Greenland shelf and fjords. The hydrographic structure of this older WGC system may, however, have been characterized by a very broad low-salinity surface layer reaching far beyond the shelf edge and originating from enhanced production of meltwater from the GIS. A similar

scenario has previously been reported for the East Greenland Current on the Southeast Greenland shelf (Kuijpers et al. 2003). Together with results from core studies in Iceland and East Greenland waters (Castañeda et al. 2004; Olafsdottir et al. 2010; Jennings et al. 2011), our data thus indicate that significant deglacial GIS melting ceased by ca. 7,700 cal. yr BP, which allowed the establishment of a modern subpolar gyre system and deep-water convection in the Labrador Sea.

We thus conclude that significant melting of the GIS should be taken into account when discussing driving mechanisms underlying the 8.2 ka event, as large-scale melting of the GIS may have contributed to a lowering of North Atlantic surface salinity prior to 8,200 cal. yr BP. Melting of the GIS was thus presumably an important factor for setting the stage for the 8.2 ka event. However, it was probably not a main driving mechanism for the 8.2 ka event itself.

7. Acknowledgements

Funding was provided by the Carlsberg Foundation (grants to HE and MFK), the Geological Survey of Denmark and Greenland (GEUS), The Danish Council for Independent Research | Nature and Universe (FNU Grants 21-04-0336 and 09-069833 to AKU and MSS), the EU FP7 project 'Past4Future' (project no. 243908), and the German Science Foundation DFG (grant MO1422/2-1 to MM). Shiptime on *RV Dana* (2000) was funded by FNU (grant to AKU), while the 2004 *Dana* cruise was financed by the Greenland Bureau of Mineral Resources, Nuuk, and GEUS. Master and crew of *RV Dana* are acknowledged for their assistance and engagement during the work at sea. We would like to thank Ian Snowball, Lund University, Sweden, for discussions on mineral magnetic parameters and supervision of measurements. We would also like to thank Ingerlise Nørgaard

499 (GEUS) and Svend Meldgaard Christiansen† (Aarhus University) for laboratory assistance. Finally,
500 we are grateful for the suggestions and comments by the two anonymous reviewers.
501
502

8. References

Alley, R.B., Mayewski, P.A., Sowers, T., Stuiver, M., Taylor, K.C., Clark, P.U., 1997. Holocene climatic instability: A prominent, widespread event 8200 years ago. Geology 25, 483–486, doi:10.1130/0091-7613(1997)025<0483:HCIAPW>2.3.CO;2.

Alley, R. B., Ágústsdóttir, A. M., 2005. The 8k event: cause and consequences of a major Holocene abrupt climate change. Quat. Sci. Rev. 24 (10-11), 1123–1149, doi:10.1016/j.quascirev.2004.12.004.

AMAP, 2009. The Greenland Ice Sheet in a Changing Climate: Snow, Water, Ice and Permafrost in the Arctic (SWIPA) 2009. By: Dahl-Jensen, D., Bamber, J., Bøggild, C.E., Buch, E., Christensen, J.H., Dethloff, K., Fahnestock, M., Marshall, S., Rosing, M., Steffen, K., R. Thomas, Truffer, M., van den Broeke, M., van der Veen, C.J., Arctic Monitoring and Assessment Programme (AMAP), Oslo, 115 pp.

Andersen, C., Koc, N., Moros, M., 2004. A highly unstable Holocene climate in the subpolar North Atlantic: Evidence from diatoms. Quat. Sci. Rev. 23, 2155–2166.

Arctic Climate Impact Assessment (ACIA), 2004. Issued by the Fourth Arctic Council Ministrerial Meeting, Reykjavik.

525 Barber, D.C., Dyke, A., Hillaire-Marcel, C., Jennings, A.E., Andrews, J.T., Kerwin, M.W.,
526 Bilodeau, G., McNeely, R., Southon, J., Morehead, M.D., Gagnon, J.M., 1999. Forcing of the cold
527 event 8200 years ago by catastrophic drainage of laurentide lakes. Nature 400, 344-348.
528
529 Be´, A.W.H., Tolderlund, D.S., 1971. Distribution and ecology of living planktonic foraminifera in
530 surface waters of the Atlantic and Indian oceans. In: Funnell, B.M., Riedel, W.R. (Eds.),
531 Micropaleontology of the Oceans. Cambridge Univ. Press, London, pp. 105–149.
532
533 Bennike, O., Björck, S. 2002. Chronology of the last recession of the Greenland Ice Sheet, J. Quat.
534 Sci., 17, 211–219, doi:10.1002/jqs.670.
535
536 Born, A., Levermann, A., 2010. The 8.2 ka event: Abrupt transition of the subpolar gyre toward a
537 modern North Atlantic circulation. Geochem. Geophys. Geosyst. 11, Q06011,
538 doi:10.1029/2009GC003024.
539
540 Came, R.E., Oppo, D.W., McManus, J.F., 2007. Amplitude and timing of temperature and salinity
541 variability in the subpolar North Atlantic over the past 10 k.y. Geology 35, 315–318.
542
543 Castañeda, I. S., Smith, L. M., Kristjánsdóttir, G. B., Andrews, J. T. 2004. Temporal changes in
544 Holocene $\delta^{18}O$ records from the northwest and central North Iceland Shelf. J. Quat. Sci. 19, 321–
545 334.
546
547 Cuny, J., Rhines, P.B., Kwok, R., 2005. Davis Strait volume, freshwater and heat fluxes. Deep-Sea
548 Res. I 52, 519-542.

549

550 Dalhoff, F., Kuijpers, A., Nielsen, T., Lassen, S., Boserup, J., Hansen, E., 2005.
551 Havbundsprøveindsampling ud for Vestgrønland H/F DANA 17/09-04/10 2004. Danmarks og
552 Grønlands Geologiske Undersøgelse, Rapport 2005/1, 44 pp.

553 Darling, K.F., Kucera, M., Kroon, D., Wade, C.M., 2006. A resolution for the coiling direction
554 paradox in *Neogloboquadrina pachyderma.* Paleoceanography 21, PA2011, 14 PP,
555 doi:10.1029/2005PA001189.

556 Dowdeswell, J.A., Cromack, M., 1991. Behaviour of a glacier-derived suspended sediment plume
557 in a small Arctic inlet. J. Geology 99 (1), 111-123.

558 Ebbesen, H., Hald, M., Eplet, T.-H., 2007. Lateglacial and Early Holocene climatic oscillation on
559 the western Svalbard margin, European Arctic. Quat. Sci. Rev. 26, 1999-2011.
560

561 Ellison, C.R.W., Chapman, M.R. Hall, I.R., 2006. Surface and deep ocean interactions during the
562 cold climate event 8200 years ago. Science 312, 1929–1932.
563

564 England, J.H., 1999. Coalescent Greenland and Innuitian ice during the Last Glacial Maximum:
565 Revising the Quaternary of the Canadian High Arctic. Quat. Sci. Rev. 18, 421-426.
566

567 England, J.H., Atkinson, N., Bednarski, J.B., Dyke, A.S., Hodgson, D.A., Cofaigh, C.Ó., 2006. The
568 Innuitian Ice Sheet: Configuration, dynamics and Chronology. Quat. Sci. Rev. 25, 689-703.
569

570 Fagel, N., C. Hillaire-Marcel, and C. Robert (1997). Changes in the Western Boundary
571 Undercurrent outflow since the Last Glacial Maximum, from smectite/illite ratios in deep Labrador
572 Sea sediments, Paleoceanography 12, 79-96.
573
574 Funder, S., Jennings, A. E., Kelly, M. J., 2004. Middle and late Quaternary glacial limits in
575 Greenland, in Quaternary Glaciations: Extent and Chronology, Part II, edited by J. Ehlers and P. L.
576 Gibbard, pp. 425–430, Elsevier, New York.
577
578 Hald, M., Steinsund, P. I., 1992. Distribution of surface sediment benthic foraminifera in the
579 southwestern Barents Sea, J. Foramin. Res. 22, 347-262.
580
581 Hall, I.R., Bianchi, G., Evans, J.R., 2004. Centennial to millenial scale Holocene climate- deep
582 water linkage in the North Atlantic. Quat. Sci. Rev. 23, 1529–1536.
583
584 Henriksen, N., Higgins, A. K., Kalsbeek, F., Pulvertaft, T. C. R. 2009: Greenland from Archaean to
585 Quaternary. Descriptive text to the 1995 Geological map of Greenland, 1:2 500 000. 2nd edition.
586 Geol. Surv. of Denmark and Greenland, Bull. 18, 126 pp. + map.
587
588 Hillaire-Marcel, C., de Vernal, A., Bilodeau, G., Weaver, A.J., 2001. Absence of deep-water
589 formation in the Labrador Sea during the last interglacial period. Nature 410, 1073-1077.
590
591 Hoffmann, G., Kuijpers, A., Thiede, J., 1999. Climate change and the Viking-age fjord environment
592 of the Eastern Settlement, SW Greenland. 'Poseidon' Cruise no. 243 Cruise Report, Reports on
593 Polar Research 331, Alfred-Wegener-Institute for Polar and Marine Research, Bremerhaven, 34 pp.
594

595 IPCC, 2007. Summary for Poicymakers, in: Climate Change 2007, The Physical Science Basis,
596 Contribution of Working Group I to the Fourth Assessment Report of the Intergovernmental Panel
597 on Climate Change, edited by: Solomon, S., Qin, D., Manning, M., Chen, Z., Marquis, M., Averyt,
598 K. B., Tignor, M., and Miller, H. L., Cambridge University Press, Cambridge, UK and New York,
599 USA.
600
601 Jansen, J.H.F., Van der Gaast, S.J., Koster, B., Vaars, A.J., 1998. CORTEX, a shipboard
602 XRFscanner for element analyses in split sediment cores. Mar. Geol. 151, 143–153.
603
604 Jennings, A, Andrews, J., Wilson, L., 2011. Holocene environmental evolution of the SE Greenland
605 Shelf North and South of the Denmark Strait: Irminger and East Greenland current interactions.
606 Quat. Sci. Rev. 30, 980-998. Doi:10.1016/j.quascirev.2011.01.016.
607
608 Jennings, A. E., Knudsen, K. L., Hald, M., Hansen, C. V., Andrews, J.T., 2002. A mid-Holocene
609 shift in Arctic sea-ice variability on the East Greenland Shelf. Holocene 12 (1), 49–58, DOI:
610 10.1191/0959683602hl519rp.
611
612 Johannesen, T., Jansen, E., Flatøy, A., Ravelo, A. C., 1994. The relationship between surface water
613 masses, oceanic fronts and paleoclimatic proxies in surface sediments of the Greenland, Iceland,
614 Norwegian Seas. in, Carbon Cycling in the Glacial Ocean: Constraints in the Ocean's Role in
615 Global Change. Quantitative Approaches in Paleoceanography, edited by Zahn, R., Pedersen, T.F.,
616 Kaminski, M.A., Labeyrie, L. Springer, New York 61-86.
617

618 Johnsen, S.J., Clausen, H.B., Dansgaard, W., Fuhrer, K., Gundestrup, N., Hammer, C.U., Iversen,
619 P., Jouzel, J., Stauffer, B., Steffensen, J.P., 1992. Irregular glacial interstadials recorded in a new
620 Greenland ice core. Nature 359, 311-313.
621
622 Johnsen, S.J., Dahl-Jensen, D., Gundestrup, N., Steffensen, J.-P., Clausen, H.B., Miller, H.,
623 Masson-Delmotte, V., Sveinbjornsdottir, A.E. White, J., 2001. Oxygen isotope and
624 palaeotemperature records from six Greenland ice-core stations: Camp Century, Dye-3, GRIP,
625 GISP2, Renland and NorthGRIP. J. Quat. Sci. 16, 299-307.
626
627 Kaufmann, D.S., Ager, T.A., Anderson, N.J., Anderson, P.M., Andrews, J.T., Bartlein, P.J.,
628 Brubaker, L.B., Coats, L.L., Cwynar, L.C., Duvall, M.L., Dyke, A.S., Edwards, M.E., Eisner, W.R.,
629 Gajewski, K., Geirsdóttir, A., Hu, F.S., Jennings, A.E., Kaplan, M.R., Kerwin, M.W., Lozhkin,
630 A.V., MacDonald, G.M., Miller, G.H., Mock, C.J., Oswald, W.W., Otto-Bliesner, B.L., Porinchu,
631 D.F., Rühland, K., Smol, J.P., Steig, E.J., Wolfe, B.B., 2004. Holocene thermal maximum in the
632 western Arctic (0-180ºW). Quat. Sci. Rev. 23, 529-560.
633
634 Keigwin, L.D., Sachs, J.P., Rosenthal, Y., Boyle, E.A., 2005. The 8200 year B.P. event in the slope
635 water system, western subpolar North Atlantic. Paleoceanography 20, doi:10.1029/2004PA001074.
636
637 Kleiven, H.F., Kissel, C., Laj, C., Ninnemann, U.S., Richter, T.O., Cortijo, E., 2008. Reduced North
638 Atlantic Deep Water coeval with the glacial Lake Agassiz fresh water outburst. Science 319, 60–64.
639

640 Klitgaard-Kristensen, D., Sejrup, H.P., Haflidason, H., Johnsen, S., Spurk, M., 1998. A regional
641 8200 cal. yr BP cooling event in northwest Europe, induced by final stages of the Laurentide ice-
642 sheet deglaciation? J. Quat. Sci. 13, 165-169.
643
644 Knudsen, K. L., Stabell, B., Seidenkrantz, M.-S., Eiríksson, J., Blake, Jr, W., 2008. Deglacial and
645 Holocene conditions of the southern Nares Strait, north Baffin Bay: sediments, foraminifera,
646 diatoms and stable isotopes. Boreas 37, 346–376, doi:10.1111/j.1502-3885.2008.00035.x.
647
648 Knutz, P.C., Sicre, M.A., Ebbesen, H., Christiansen, S., Kuijpers, A., 2011. Multiple-stage deglacial
649 retreat of the southern Greenland Ice Sheet linked with Irminger Current warm water transport,
650 Paleoceanography, 26, PA3204, doi:10.1029/2010PA002053.
651
652 Kobashi, T., Severinghaus, J. P., Brook, E. J., Barnola, J.-M., Alexi M. Grachev, A. M., 2007.
653 Precise timing and characterization of abrupt climate change 8200 years ago from air trapped in
654 polar ice. Quat. Sci. Rev. 26, 1212-1222, doi:10.1016/j.quascirev.2007.01.009.
655
656 Korsun, S., Hald, M., 2000. Seasonal dynamics of benthic foraminifera in a glacially fed fjord of
657 Svaldbard, European arctic. J. Foramin. Res. 30 (4), 251-271.
658
659 Kuijpers, A., Abrahamsen, N., Hoffmann, G., Hühnerbach, V., Konradi, P., Kunzendorf, H.,
660 Mikkelsen, N., Thiede, J., Weinrebe, W., 1999. Climate change and the Viking-age fjord
661 environment of the Eastern Settlement, South Greenland. Geology of Greenland Survey Bull. 183,
662 61-67.
663

664 Kuijpers, A., Lloyd, J.M., Jensen, J.B., Endler, R., Moros, M., Park, L.A., Schulz, B., Jensen, K.G.,
665 Laier, T., 2001. Late Quaternary circulation changes and sedimentation in Disko Bugt and adjacent
666 fjords, central West Greenland. Geology of Greenland Survey Bull. 189, 41–47.
667
668 Kuijpers, A., Troelstra, S.R., Prins, M.A., Linthout, K., Akhmetzhanov, A., Bouryak, S.,
669 Bachmann, M.F., Lassen, S., Rasmussen, T., Jensen, J.B., 2003. Late Quaternary sedimentary
670 processes and ocean circulation changes at the Southeast Greenland margin. Mar. Geol. 195, 109-
671 129.
672
673 Lassen, S.J., Kuijpers, A., Kunzendorf, H., Hoffmann-Wieck, G., Mikkelsen, N., Konradi, P., 2004.
674 Late-Holocene Atlantic bottom-water variability in Igaliku Fjord, South Greenland, reconstructed
675 from foraminifera faunas. Holocene 14, 2, 165-171.
676
677 Leverington, D.W., Mann, J.D., Teller, J.T., 2002. Changes in the bathymetry and volume of glacial
678 Lake Agassiz between 9200 and 7700 14C yr BP. Quat. Res. 57, 244-252.
679
680 Long, A.J., Roberts, D.H., Dawson, S., 2006. Early Holocene history of the west Greenland Ice
681 Sheet and the GH-8.2 event, Quat. Sci. Rev. 25, 904–922.
682
683 Long, A.J., Woodroffe, S.A., Roberts, D.H., Dawson, S. 2011. Isolation basins, sea-level changes
684 and the Holocene history of the Greenland Ice Sheet. Quat. Sci. Rev. 30, 3748-3768.
685
686 Lloyd, J.M., Park, L.A., Kuijpers, A. and Moros, M. 2005: Early Holocene palaeoceanography and
687 deglacial chronology of Disko Bugt, West Greenland. Quat. Sci. Rev. 24, 1741_/55.

688

689 Lloyd, J. M., Moros, M., Perner, K., Telford, R.J., Kuipers, A., Jansen, E., McCarthy, D. 2011. A
690 100 yr record of ocean temperature control on the stability of Jacobshavn Isbrae, West Greenland.
691 Geology, in press.

692

693 McGregor, V.R., 1993. Descriptive text to 1:100,000 sheet Qôrqut 64 V.1, Geological map of
694 Greenland. SydGrønlands Geologisk Undersøgelse, pp. 37–38.

695

696 Mernild, S.H., Seidenkrantz, M.-S., Chylek, P., Liston, G.E., Hasholt, B., 2012. Climate driven
697 fluctuations in simulated freshwater runoff to Sermilik Fjord, East Greenland, during the last 4000
698 years. Holocene, in press, doi: 10.1177/0959683611431215.

699

700 Moros, M., Jensen, K.G., Kuijpers, A., 2006. Mid to late-Holocene variability in Disko Bugt,
701 central West Greenland. Holocene 16, 357–367.

702

703 Møller, H.S., Jensen, K.G., Kuijpers, A., Aagaard-Sørensen, S., Seidenkrantz, M.-S., Endler, R. and
704 Mikkelsen, N., 2006. Late Holocene environmental and climatic changes in Ameralik Fjord,
705 Southwest Greenland – evidence from the sedimentary record. Holocene 16, 685-695.

706

707 Mudie, P.T., Rochon, A., Prins, M.A., Soenarjo, D., Troelstra, S.R., Levac, E., Scott, D.B.,
708 Roncaglia, L., Kuijpers, A., 2004 (published 2006). Late Pleistocene-Holocene Marine Geology of
709 Nares Strait Region. Palaeoceanography from Foraminifera and Dinoflagellate Cysts,
710 Sedimentology and Stable Istopes. Polarforschung 74 (1-3), 169-183.

711

712 Nick, F. M., Vieli, A., Howat, I. M., Joughin, I., 2009. Large-scale changes in Greenland outlet
713 glacier dynamics triggered at the terminus. Nature Geoscience 2, 110-114, doi:10.1038/ngeo394.
714
715 Olafsdottir, S., Jennings, A.E., Geirsdottir, A., Andrews, J.T., Miller, G.H., 2010. Holocene
716 variability of the North Atlantic Irminger Current on the South- and Northwest shelf of Iceland.
717 Mar. Micropaleontol. 77, 101e118.
718
719 Ostermann, D.R., Curry, W.B., 2000. Calibration of stable isotopic data: An enriched $\delta^{18}O$ standard
720 used for source gas mixing detection and correction. Paleoceanography 15, 353-360.
721
722 Overpeck, J., Hughen, K., Hardy, D., Bradley, R., Case, R., Douglas, M., Finney, B., Gajevski, K.,
723 Jacoby, G., Jennings, A., Lamoureux, S., Lasca, A., MacDonald, G., Moore, J., Retelle, M., Smith,
724 S., Wolfe, A., Zielinski, G., 1997. Arctic environmental change of the last four centuries. Science
725 278, 1251-1256.
726
727 Ramsey, C. B., 2008. Deposition models for chronological records. Quat. Sci. Rev. 27(1-2): 42-60.
728
729 Reimer, P. J., Reimer, R. W., 2001. A marine reservoir correction database and on-line interface.
730 Radiocarbon 43, 461-463.
731
732 Reimer, P. J., Baillie, M. G. L., Bard, E., Bayliss, A., Beck, J. W., Blackwell, P. G., Bronk Ramsey,
733 C., Buck, C. E., Burr, G. S., Edwards, R. L., Friedrich, M., Grootes, P. M., Guilderson, T. P.,
734 Hajdas, I., Heaton, T. J., Hogg, A. G., Hughen, K. A., Kaiser, K. F., Kromer, B., McCormac, F. G.,
735 Manning, S. W., Reimer, R. W., Richards, D. A., Southon, J. R., Talamo, S., Turney, C. S. M., van

736 der Plicht, J., Weyhenmeyer, C. E., 2009. IntCal09 and Marine09 radiocarbon age calibration
737 curves, 0-50,000 years cal BP. Radiocarbon, 51(4), 1111-1150.
738
739 Ren, J., Jiang, H., Seidenkrantz, M.-S. & Kuijpers, A., 2009. A diatom-based reconstruction of
740 Early Holocene hydrographic and climatic change in a southwest Greenland fjord. Mar.
741 Micropalaeontol. 70, 166–176, doi:10.1016/j.marmicro.2008.12.003.
742
743 Rignot, E., Kanagaratnam, P., 2006. Changes in the Velocity Structure of the Greenland Ice Sheet.
744 Science 311, 986 – 990.
745
746 Rignot, E., Velicogna, I., van den Broeke, M. R., Monaghan, A., Lenaerts, J., 2011. Acceleration of
747 the contribution of the Greenland and Antarctic ice sheets to sea level rise. Geophys. Res. Lett. 38,
748 L05503, doi:10.1029/2011gl046583 .
749
750 Rinterknecht, V., Gorokhovich, Y., Schaefer, J., Caffee, M., 2009., Preliminary ^{10}Be chronology for
751 the last deglaciation of the western margin of the Greenland Ice Sheet, J. Quat. Sci. 24, 270–278,
752 doi:10.1002/jqs.1226.
753
754 Risebrobakken, B., Jansen, E., Andersson, C., Mjelde, E., Hevrøy, K., 2003. A high-resolution
755 study of Holocene paleoclimatic and paleoceanographic changes in the Nordic Seas. Paleoceanogr.
756 18 (1), 1-14.
757

758 Roberts, D. H., Long, A. J., Schnabel, C., Davies, B. J., Xu, S., Simpson, M. J. R., Huybrechts, P.,
759 2009. Ice sheet extent and early deglacial history of the southwestern sector of the Greenland Ice
760 Sheet. Quat. Sci. Rev. 28, 2760–2773, doi:10.1016/j.quascirev.2009.07.002.
761
762 Rohling, E.J., Pälike, H., 2005. Centennial-scale climate cooling with a sudden cold event around
763 8,200 years ago. Nature 434, 975-979.
764
765 Rytter, F., Knudsen, K. L., Seidenkrantz, M.-S., Eiríksson, J., 2002. Modern distribution of benthic
766 foraminifera on the North Icelandic shelf and slope. J. Foramin. Res. 32, 217-244.
767
768 Sachs, J.P., 2007. Cooling of Northwest Atlantic slope waters during the Holocene, Geophys. Res.
769 Lett. 34, L03609, doi:10.1029/2006GL028495.
770
771 Sarnthein, M., Van Kreveld, S., Erlenkeuser, H., Grootes, P. M., Kucera, M., Pflaumann, U.,
772 Schulz, M., 2003. Centennial-to-millennial-scale periodicities of Holocene climate and sediment
773 injections off the western Barents shelf, 75°N. Boreas 32, 448-461.
774
775 Seidenkrantz, M.-S., 1995. *Cassidulina teretis* Tappan and *Cassidulina neoteretis* new species
776 (Foraminifera): stratigraphic markers for deep sea and outer shelf areas. J. Micropalaeontol. 14,
777 145-157.
778
779 Seidenkrantz, M.-S., Aagaard-Sørensen, S., Sulsbrück, H., Kuijpers, A., Jensen, K.G., Kunzendorf,
780 H., 2007. Hydrography and climate of the last 4400 years in a SW Greenland fjord: implications for
781 Labradors Sea Palaeoceanography. Holocene 17, 3, 387-401.

782

783 Snowball, I., Moros, M., 2003. Saw-tooth pattern of North Atlantic current speed during
784 Dansgaard_/Oeschger cycles revealed by the magnetic grain size of Reykjanes Ridge sediments at
785 598 N. Palaeoceanography 18, 1026, doi:10.1029/2001PA000732.

786

787 Steffen, K., S.V. Nghiem, S.V., Huff, R., Neumann, G., 2004. The melt anomaly of 2002 on the
788 Greenland Ice Sheet from active and passive microwave satellite observations. Geophys. Res. Lett.,
789 31(20), L2040210.1029/2004GL020444.

790

791 Steinsund, P.I., Polyak, L., Hald, M., Mikhailov, V., Korsun, S., 1994. Distribution of calcareous
792 benthic foraminifera in recent sediments of the Barents and Kara Sea. In Steinsund, P.I., Benthic
793 foraminifera in surface sediments of the Barents and Kara Seas: modern and late Quaternary
794 application. Ph.D. thesis, Department of Geology, Institute of Biology and Geology, University of
795 Tromsø, Norway.

796

797 Steenfelt, A., 1990. Regional compilations of geoscience data from the Nuuk-Manitsoq area,
798 Southern West Greenland. GGU. Thematic Map Series.

799

800 Stoner, J.S. and Andrews, J.T. 1999: The North Atlantic as a Quaternary magnetic archive. In
801 Maher, B.A. and Thompson, R., editors, Quaternary climates, environments and magnetism.
802 Cambridge University Press, 49 /80.

803

804 Stuiver, M., Reimer, P.J., Braziunas, T.F., 1998. High-precision radiocarbon age calibration for
805 terrestrial and marine samples. Radiocarbon 40, 1127-51.

Tang, C.C.L., Ross, C.K., Yao, T., Petrie, B., DeTracey, B.M., Dunlap, E., 2004. The circulation, water masses and sea- ice of Baffin Bay. Progress in Oceanography 63, 183-228.

Verosub, K.L., Roberts, A.P. 1995. Environmental magnetism: past, present, and future. J. Geophys. Res. 100, 2175_/92.

Wagner F., Aaby, B., Visscher, H., 2002. Rapid atmospheric CO2 changes associated with the 8,200-years-B.P. cooling event. Proc. Natl. Acad. Sci. USA 99 (19), 12011–12014, doi:10.1073_pnas.182420699.

816 **Figure captions**

817

818 **Figure 1.** Location map of the study region. The modern surface ocean circulation is mainly
819 influenced by waters from the East Greenland Current (EGC) and the West Greenland Current
820 (WGC). At the surface, the WGC transports cold, low-salinity water masses including glacial
821 meltwater and Polar Water derived from the EGC. At greater water depths (> 150-200 m), the
822 WGC entrains warmer, saline Atlantic water-masses (Irminger Sea Water) derived from the
823 Irminger Current (IC). NADW: North Atlantic Deep Water. The investigated marine sediment cores
824 were collected at four sites off West Greenland. Two of the sites are located in the Disko Bugt area
825 (DA00-04P and DA00-06P), while one core site is located in Ameralik Fjord (DA04-41P) near
826 Nuuk. These core data were compared with a lower-resolution planktonic foraminiferal record from
827 the northernmost Labrador Sea basin (DA04-31P).

828

829 **Figure 2**. Age models for cores DA06P, DA04P, DA31P and DA41P. The age models are based on
830 calibrated ^{14}C datings, the OxCal 4.1 program, and correlation with the Greenland ice core
831 chronology.

832

833 **Figure 3.** Magnetic susceptibility (χ) and χ_{ARM}/χ ratios as well as >63 µm and >150 µm grain size
834 fractions (in % of the total sediment) from cores DA06P and DA04P. For explanation, see text
835 (Results and palaeoenvironment).

836

837 **Figure 4.** A detailed study of the early Holocene from core DA04-41P, illustrating magnetic
838 susceptibility (χ), χ_{ARM}/χ ratios, the >63 µm grain size fraction (% of the total sediment), the

elements Fe (Iron), K (Potassium), Ti (Titanium), Ca (Calcium) and Br (Bromium) measured in cps (counts per second, x1000 or x100).

Figure 5. A detailed record of the early Holocene from core DA04-41P, illustrating the occurrence of the most important benthic foraminiferal species (%), as well as the benthic foraminiferal fluxes (no. specimens/year). Magnetic susceptibility (χ) values are shown for comparison. Due to extreme surface water characteristics associated with meltwater outflow, the planktonic foraminiferal fauna in these cores is extremely scant or non-existent.

Figure 6. A detailed record of the planktonic foraminifera, production of planktonic foraminifera (numbers/gram sediment) and stable oxygen and carbon isotopes (measured in PDB) in core DA04-31P, during the period from 10,000-6,000 cal. yr BP.

Table caption

Table 1. Studied marine sediment cores.

Table 2. An overview of the AMS ^{14}C dates and age correlation of the studied sediment cores. The individual age models for each core were performed by using OxCal 4.1 depositional models. The AMS ^{14}C dates are to shown in Table 2. The radiocarbon ages were converted into calibrated years by using OxCal 4.1 (Ramsey 2008) and the marine calibration curve, marine09 (Reimer et al. 2009) with local reservoir ages ΔR.

Figure

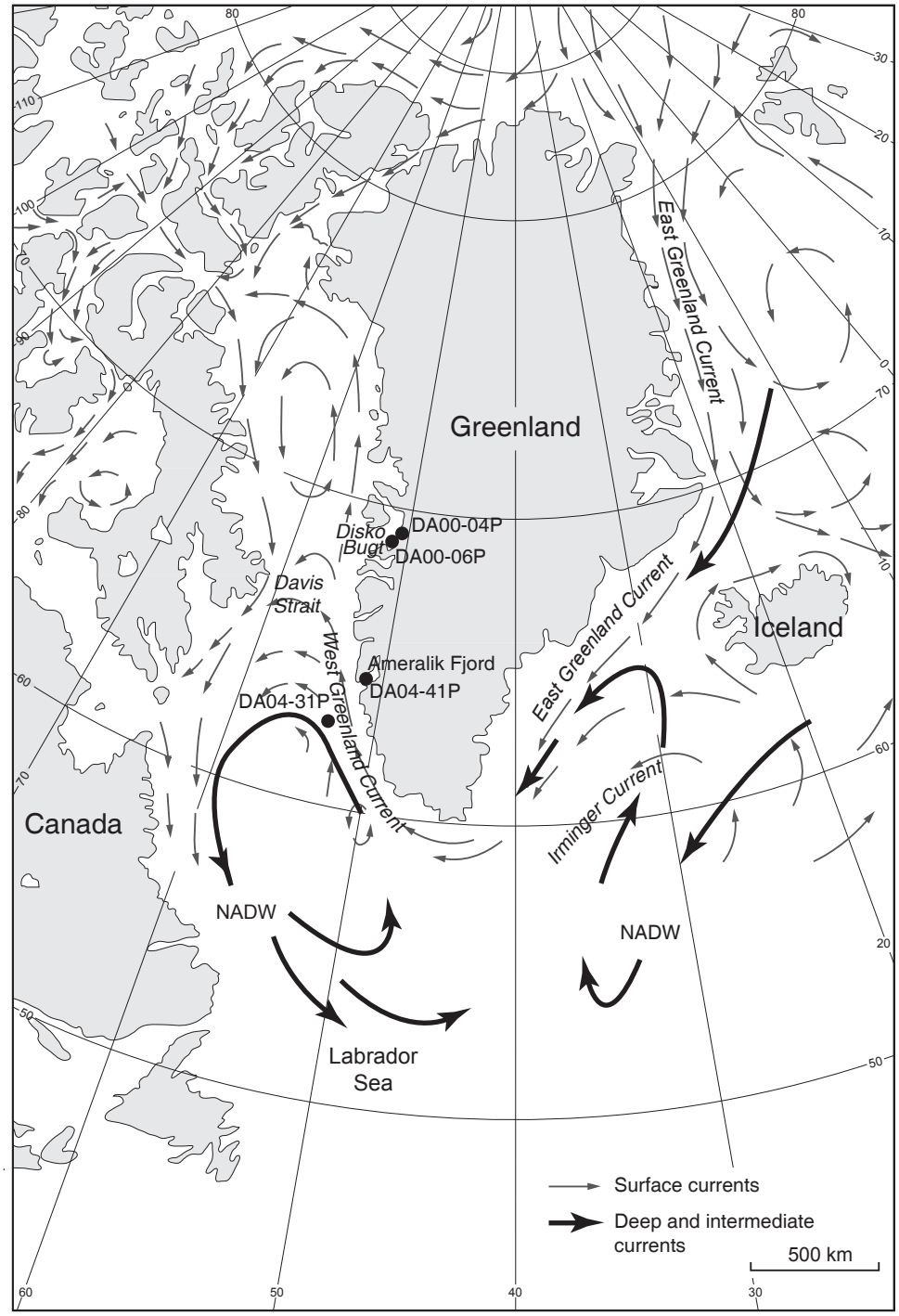
Greenland
Iceland
Canada
East Greenland Current
East Greenland Current
West Greenland Current
Irminger Current
Disko Bugt
DA00-04P
DA00-06P
Davis Strait
Ameralik Fjord
DA04-41P
DA04-31P
NADW
NADW
Labrador Sea
Surface currents
Deep and intermediate currents
500 km

Figure

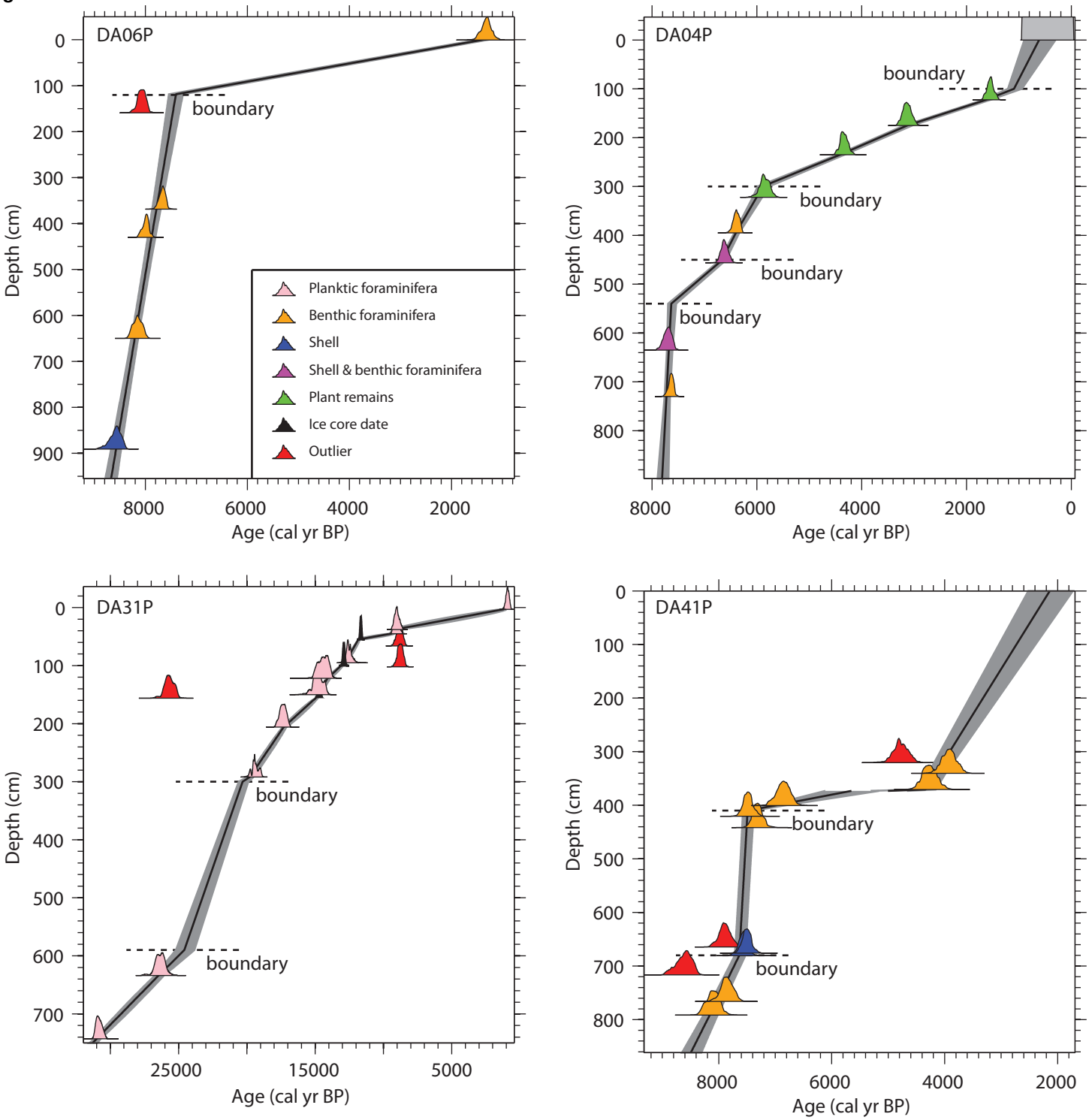
DA06P
boundary
Depth (cm)
Age (cal yr BP)
Planktic foraminifera
Benthic foraminifera
Shell
Shell & benthic foraminifera
Plant remains
Ice core date
Outlier
DA04P
boundary
boundary
boundary
boundary
DA31P
boundary
boundary
DA41P
boundary
boundary

Figure

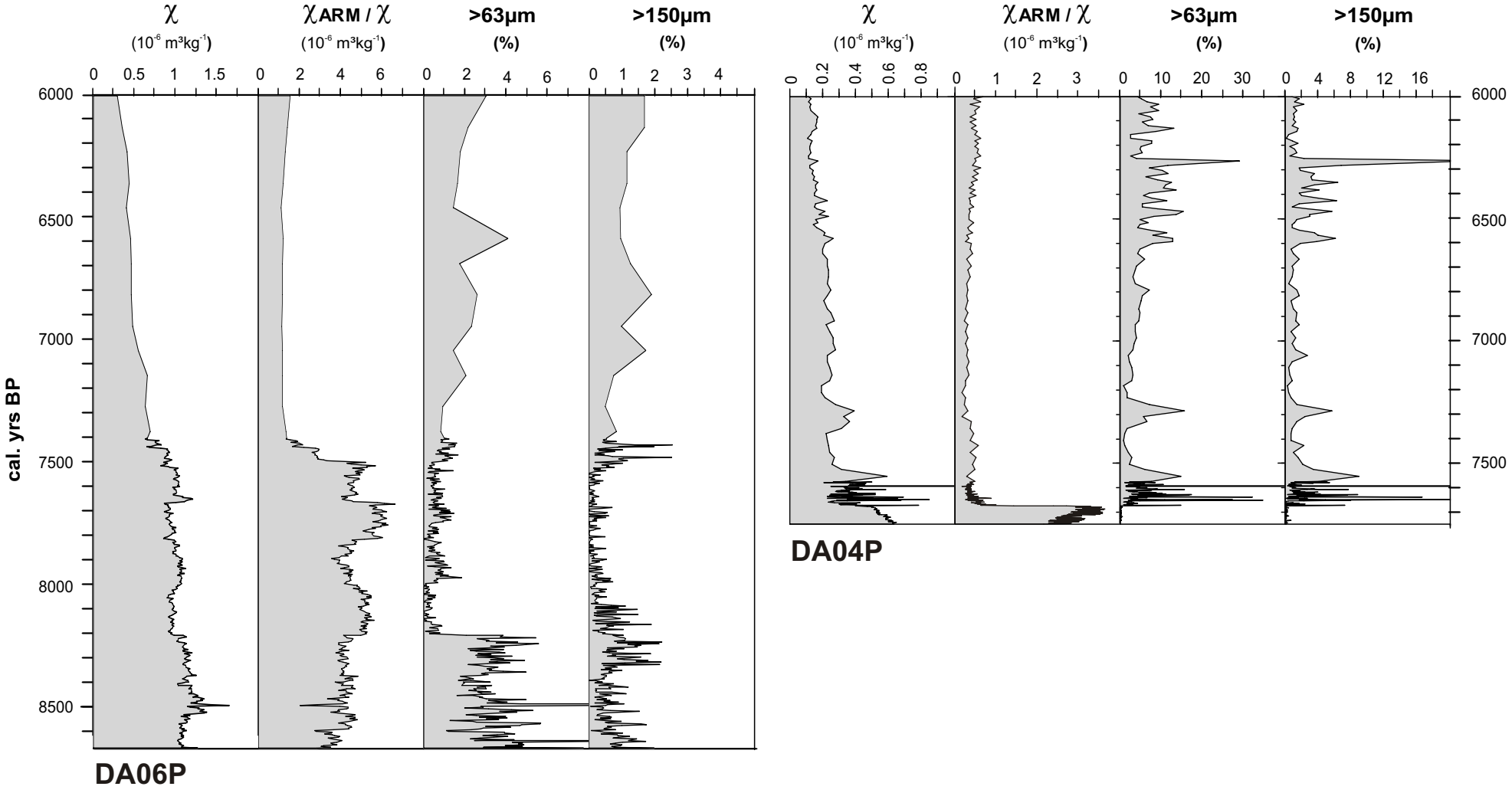
χ
(10⁻⁶ m³kg⁻¹)
χARM / χ
(10⁻⁶ m³kg⁻¹)
>63µm
(%)
>150µm
(%)
cal. yrs BP
6000
6500
7000
7500
8000
8500
DA06P
DA04P

Figure

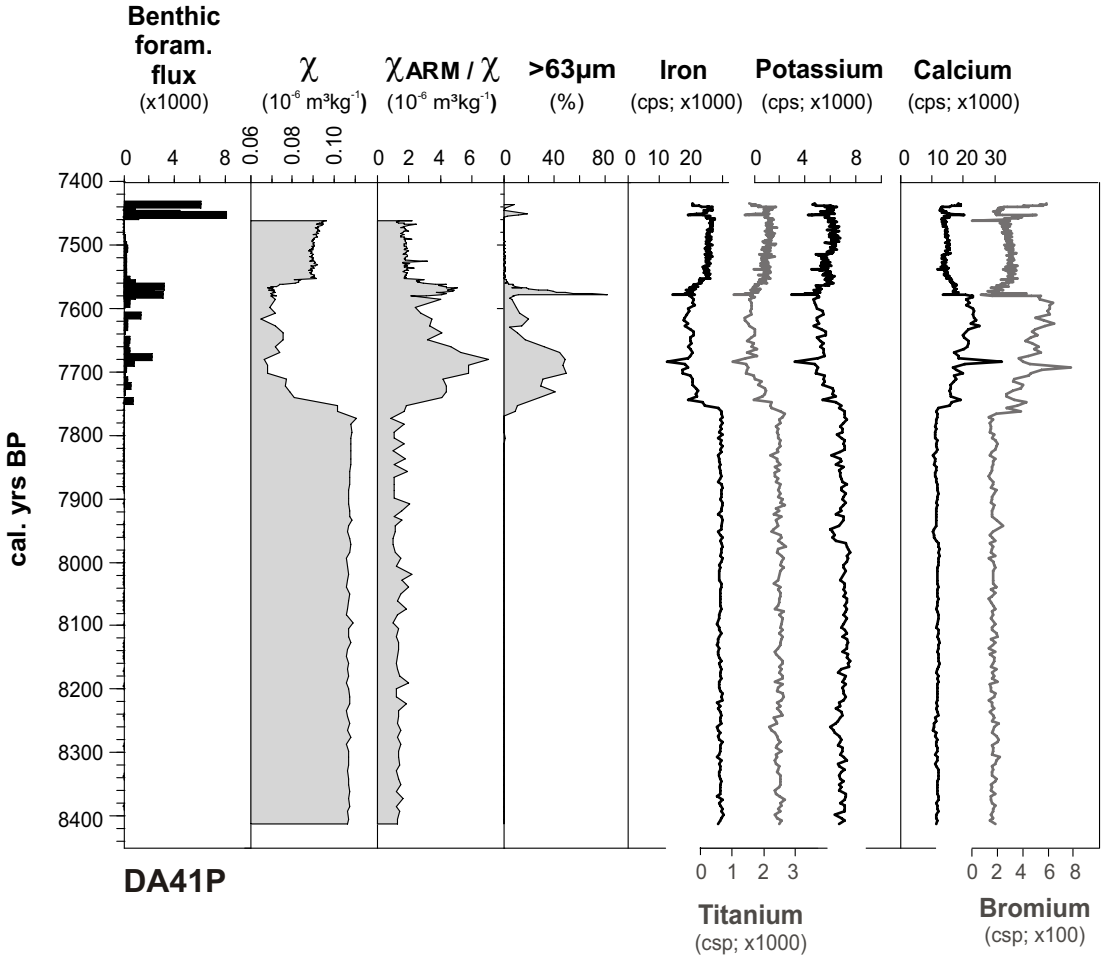
Benthic foram. flux
(x1000)
χ
(10⁻⁶ m³kg⁻¹)
χARM / χ
(10⁻⁶ m³kg⁻¹)
>63µm
(%)
Iron
(cps; x1000)
Potassium
(cps; x1000)
Calcium
(cps; x1000)
cal. yrs BP
DA41P
Titanium
(csp; x1000)
Bromium
(csp; x100)

Figure

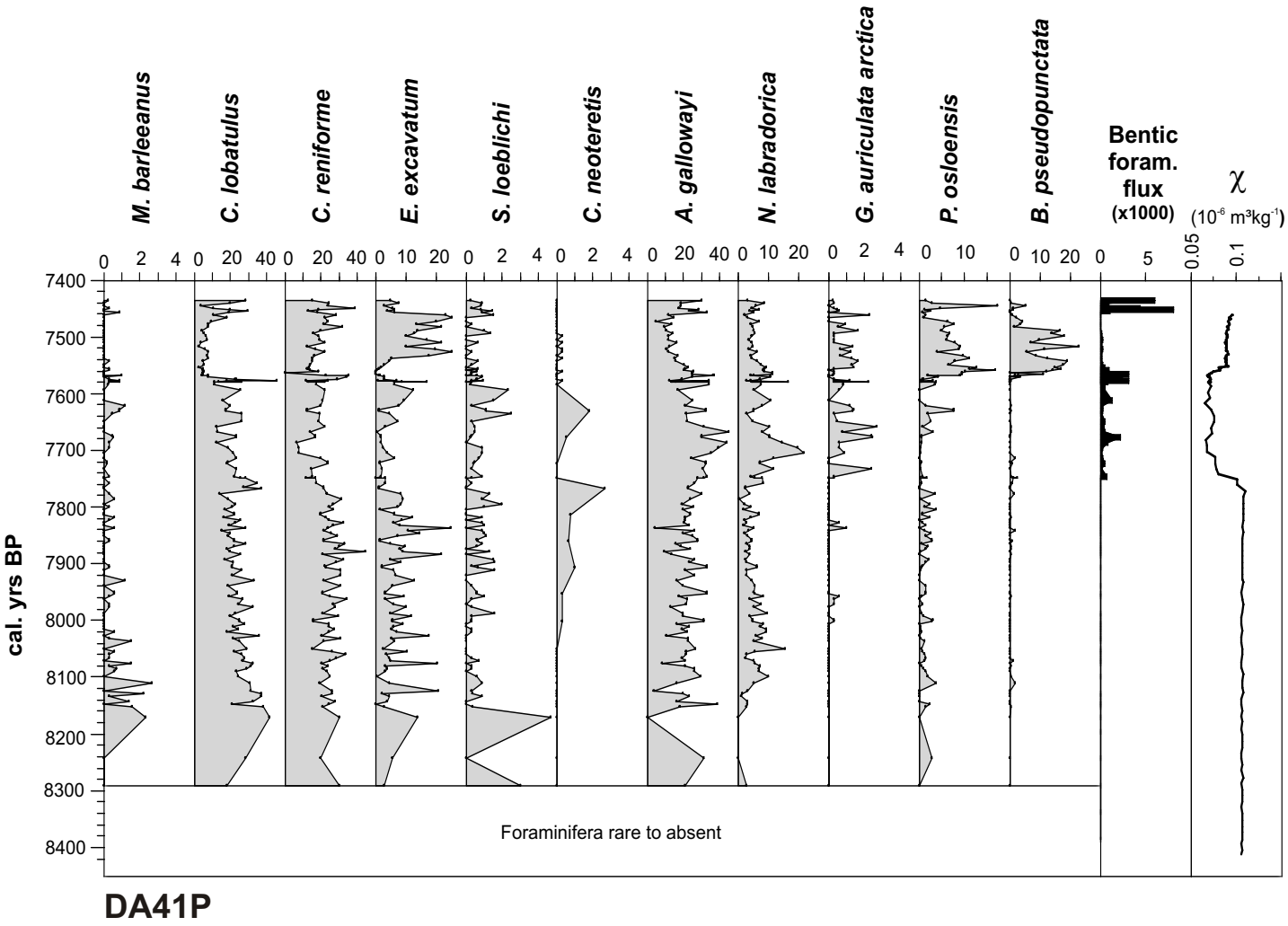
M. barleeanus
C. lobatulus
C. reniforme
E. excavatum
S. loeblichi
C. neoteretis
A. gallowayi
N. labradorica
G. auriculata arctica
P. osloensis
B. pseudopunctata
Bentic foram. flux (x1000)
χ (10⁻⁶ m³kg⁻¹)
cal. yrs BP
7400
7500
7600
7700
7800
7900
8000
8100
8200
8300
8400
Foraminifera rare to absent
DA41P

Figure

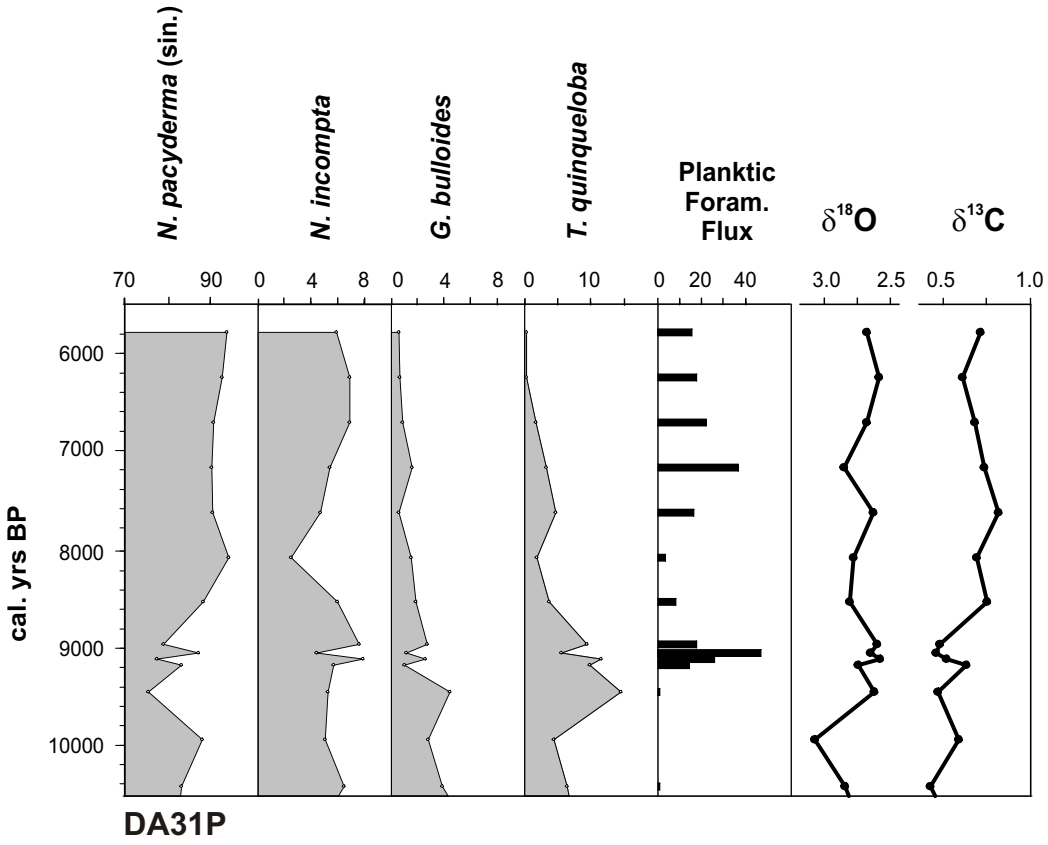
N. pacyderma (sin.)
N. incompta
G. bulloides
T. quinqueloba
Planktic Foram. Flux
δ18O
δ13C
70
90
0
4
8
0
4
8
0
10
0
20
40
3.0
2.5
0.5
1.0
6000
7000
8000
9000
10000
cal. yrs BP
DA31P

Table 1. Studied marine sediment cores

Core name	Area	Latitude	Longitude	Water depth (m)	Core length (cm)	References
DA00-06P	Disko Bugt	69°10.21N	51°23.71W	363 m	960 cm	Lloyd et al. (2005)
DA00-04P	Kangersuneq Fjord	68°44.22N	51°00.63W	265 m	890 cm	Kuijpers et al. (2001)
DA04-31P	N. Labrador Sea	62°33.775N	54°30.216W	2525 m	877 cm	Knutz et al. (in press)
DA04-41P	Ameralik Fjord	64°5.433N	51°15.530W	744 m	850 cm	Ren et al. (2009)

Table

Click here to download Table: Table 2_Final.doc

Table 2. Radiocarbon dates and calibrated ages

Core ID (water depth)	Core depth (cm)	Laboratory reference	Material dated	^{14}C age	ΔR. (yrs)	Posterior 95% conf. int. (cal. yr BP)	Age used (cal. yr BP)	References
DA00-06	0.5	KIA17925	Bentic foram. fauna	1900±90	140±30	1117-1549	1333	Lloyd et al., 2005
(363m)	159	AAR6837	Bivalve	7750±68	140±30			
	370	Poz-42499	Bentic foram. fauna	7340±50	140±30	7931-7612	7783	
	430	KIA23024	Bentic foram. fauna	7670±47	140±30	7858-8112	7982	ΔR ref=Lloyd et al. 2011
	650	KIA23025	Benthic foram. fauna	7830±70	140±30	8134-8352	8245	
	891	AAR6839	Bivalve	8243±72	140±30	8370-8715	8537	
	Core lenght: 955 cm							
DA00-04	120-125	Poz-8110	Plant remains (sea grass)	2125±35	140±30	1438-1691	1567	
(256m)	175	AAR-9810	Plant remains (sea grass)	3432±44	140±30	2924-3228	3072	
	235	Poz-8109	Plant remains (sea grass)	4380±40	140±30	4220-4500	4354	
	322	AAR-7513	Plant remains (sea grass)	5620±70	140±30	5785-6144	5946	
	390-400	Poz-8141	Benthic foram. fauna	6120±40	140±30	6262-6442	6340	Present study
	456	Poz-8143	Shell+Benthic foram. fauna	6320±40	140±30	6550-6775	6661	(Kuijpers and Moros, unpubl)
	635	Poz-8168	Shell+Benthic foram. fauna	7370±70	140±30	7513-7730	7620	ΔR ref=Lloyd et al. 2011
	730	KIA23366	Benthic foram. fauna	7310±40	140±30	7572-7775	7665	
	Core length: 897.5							
DA04-31P	0-6	AAR-10681	Planktic foram. fauna	1365±40	0±100	749-1219	988	Knutz et al. 2011
(2525m)	38	AAR-9982	Planktic foram. fauna	8420±65	0±100	8626-9256	8988	
	44-46	AAR-10456	Planktic foram. fauna	8440±55	0±100	8904-9446	9208	
	66	AAR-10682	Planktic foram. fauna	8272±47	0±100			
	94-96	AAR-10703	Planktic foram. fauna	11080±65	0±100	12423-12756	12596	
	102	AAR-9983	Planktic foram. fauna	8230±55	0±150			
	122	AAR-10820	Planktic foram. fauna	12710±260	0±150	13522-14151	13867	
	150	AAR-10683	Planktic foram. fauna	13020±65	0±150	14361-14808	14600	
	156	AAR-9984	Planktic foram. fauna	21880±170	0±150			
	206	AAR-9985	Planktic foram. fauna	14660±90	0±150	16814-17370	17081	
	292	AAR-10684	Planktic foram. fauna	16670±100	0±150	19210-20030	19556	
	634	AAR-9986	Planktic foram. fauna	22320±170	0±150	25610-26870	26242	
	743	AAR-10685	Planktic foram. fauna	26550±250	0±150	30351-31157	30769	
	Core length: 877.5 cm							
DA04-41P	320-321	AAR-11199	Benthic foram. fauna	4709±43	129±84	4580-5141	4871	ΔR ref = Reimer & Reimer 2001
(744m)	340-341	AAR-10227	Benthic foram. fauna	4061±39	129±84	3810-4355	4096	Ren et al. 2009
	370-371	AAR-11200	Benthic foram. fauna	4318±41	129±84	3969-4559	4284	
		HIATUS						
	400-401	AAR- 19624	Benthic foram. fauna	6507±48	129±84	6680-7201	6952	
	420-421	AAR-19625	Benthic foram. fauna	7115±49	129±84	7258-7601	7440	
	441-442	AAR-10228	Benthic foram. fauna	6920±42	129±84	7272-7611	7451	
	664-665	AAR-19651	Benthic foram. fauna	7565±55	129±84			
	675,5-676,5	AAR-10110	Shell (*Colus holboelli*)	7139±43	129±84	7408-7745	7579	
	680-681	AAR-10111	Shell (*Bathyarca glacialis*)	7208±43	129±84	7412-7750	7583	
	716-717	AAR-10226	Shell (Gastropoda)	8240±50	129±84			
	765-767	AAR-10792	Benthic foram. fauna	7525±65	129±84	7766-8176	7979	
	790-793	AAR-10662	Benthic foram. fauna	7765±75	129±84	7870-8335	8105	
	Core lenght: 861.5 cm							